Synchrotron Infrared Measurements of Protein Phosphorylation in Living Single PC12 Cells during Neuronal Differentiation

ARTICLE *in* ANALYTICAL CHEMISTRY · APRIL 2012

Impact Factor: 5.64 · DOI: 10.1021/ac300308x · Source: PubMed

7 AUTHORS, INCLUDING:

Hoi-ying Holman
Lawrence Berkeley National Laboratory
92 PUBLICATIONS **1,937** CITATIONS
SEE PROFILE

Zhao Hao
University of California, Berkeley
70 PUBLICATIONS **3,025** CITATIONS
SEE PROFILE

Michael C Martin
Lawrence Berkeley National Laboratory
194 PUBLICATIONS **5,960** CITATIONS
SEE PROFILE

Chengbiao Wu
University of California, San Diego
43 PUBLICATIONS **2,132** CITATIONS
SEE PROFILE

analytical chemistry

Article

pubs.acs.org/ac

Synchrotron Infrared Measurements of Protein Phosphorylation in Living Single PC12 Cells during Neuronal Differentiation

Liang Chen,[†] Hoi-Ying N. Holman,*[,†] Zhao Hao,[†] Hans A. Bechtel,[†] Michael C. Martin,[†] Chengbiao Wu,[‡] and Steven Chu*[,§,∥,⊥]

[†]Lawrence Berkeley National Laboratory, 1 Cyclotron Road, Berkeley, California 94720, United States

[‡]Department of Neurosciences, University of California at San Diego School of Medicine, La Jolla, California 92093, United States

[§]Departments of Physics and Molecular and Cell Biology, University of California at Berkeley, Berkeley, California 94720, United States

[∥]California Institute for Quantitative Biosciences (QB3), University of California at Berkeley, Berkeley, California 94720, United States

Supporting Information

ABSTRACT: Protein phosphorylation is a post-translational modification that is essential for the regulation of many important cellular activities, including proliferation and differentiation. Current techniques for detecting protein phosphorylation in single cells often involve the use of fluorescence markers, such as antibodies or genetically expressed proteins. In contrast, infrared spectroscopy is a label-free and noninvasive analytical technique that can monitor the intrinsic vibrational signatures of chemical bonds. Here, we provide direct evidence that protein phosphorylation in individual living mammalian cells can be measured with synchrotron radiation-based Fourier transform-infrared (SR-FT-IR) spectromicroscopy. We show that PC12 cells stimulated with nerve growth factor (NGF) exhibit statistically significant temporal variations in specific spectral features, correlating with changes in protein phosphorylation levels and the subsequent development of neuron-like phenotypes in the cells. The spectral phosphorylation markers were confirmed by bimodal (FT-IR/fluorescence) imaging of fluorescently marked PC12 cells with sustained protein phosphorylation activity. Our results open up new possibilities for the label-free real-time monitoring of protein phosphorylation inside cells. Furthermore, the multimolecule sensitivity of this technique will be useful for unraveling the associated molecular changes during cellular signaling and response processes.

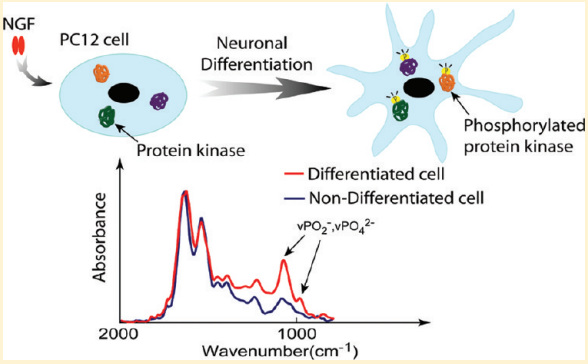

Protein phosphorylation is a reversible biochemical process in which a phosphate group is enzymatically added to serine, threonine, or tyrosine residues in protein macromolecules. This ubiquitous post-translational modification plays a pivotal role in the regulation of many important cellular processes including metabolism, cell cycling, apoptosis, proliferation, and differentiation.[1,2] For example, in neurobiology, the phosphorylation cascade of members in the mitogen activated protein kinase (MAPK) family mediates the retrograde survival response in dorsal root ganglion neurons[3] and dictates the differentiation fate of cortical progenitor cells.[4] The label-free and in situ detection of protein phosphorylation allows one to gain insights into the mechanisms underpinning these cellular processes in neurons.

The routine imaging method for detecting protein phosphorylation in individual cells employs fluorescently labeled antibodies that bind specifically to phosphorylated protein substrates.[5,6] Although highly specific and sensitive, the technique cannot examine phosphorylation changes in single cells in real time due to a reliance on cell fixation and permeabilization procedures. Another technique uses genetically encoded fluorescent protein phosphorylation reporters to directly visualize protein phosphorylation in living cells[7−9] by monitoring changes in fluorescence resonance energy transfer (FRET). However, the expression of these exogenous probes after gene delivery necessarily competes with endogenous kinase substrates and has the potential to alter the intrinsic signaling networks.[10] Moreover, knowledge of the protein sequence and structure is also a prerequisite before those two methods can be applied. Surface enhanced Raman scattering (SERS) has been used to detect the phosphorylation of surface and intracellular proteins in fixed cells[11] and native chemical constituents, such as nucleic acids and amino acids, in living cells.[12] However, the introduction of colloidal nanoparticles into a cell may induce undesired behavioral changes.[13] Conventional Raman spectroscopy has been used to probe

Received: January 31, 2012
Accepted: April 2, 2012
Published: April 2, 2012

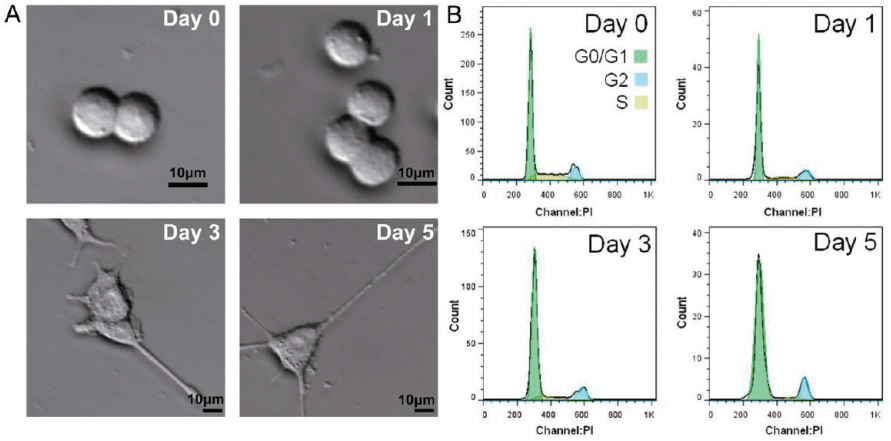

Figure 1. (A) Bright field images of PC12 cells in 1 week treatment with NGF. Pictures were taken at the 0, 24, 72, and 120 h, respectively. PC12 cells began to develop neurites longer than one cell body length at day 3. Scale bars: 10 μm. (Note: the scale of the bottom two images are twice that of the top images.) (B) Cell cycling analysis of PC12 cells treated with NGF in 1 week. The percentage of cells in G_0/G_1, G_2, and S phase at each time point were measured by fluorescence activated cell sorting (FACS) analysis with propidium iodide (PI) staining. At day 0, G1/G0 = 65.36%, G2 = 11.93%, S = 22.71%; at day 1, G1/G0 = 71.53%, G2 = 13.69%, S = 14.78%; at day 3, G1/G0 = 77.05%, G2 = 9.49%, S = 13.46%; at day 5, G1/G0 = 81.64%, G2 = 5.56%, S = 12.8%. Notice that the observed flattening of the cell body and larger cell surface area in differentiated PC12 cells are consistent with those previously reported.[32]

living cells,[14,15] but we are not aware of its application to protein phosphorylation.

In contrast, FT-IR spectroscopy with a thermal source is a label-free and nondestructive analytical technique that can identify functional groups in biomolecules by their characteristic vibrational modes.[16] It provides a wealth of chemical information about the sample without a priori knowledge.[17] FT-IR spectroscopy has been previously used to probe the phosphorylation state of residues in protein macromolecules in vitro.[18−20] When combined with an IR microscope, FT-IR spectroscopy has been used to obtain spatially resolved chemical information of fixed tissue sections[21,22] and nonfixed and hydrated cells.[23,24]

However, FT-IR spectromicroscopy with a thermal source is limited by spatial resolution and a signal-to-noise ratio (SNR) trade-off due to its low-brightness.[25] To achieve truly diffraction-limited spatial resolution with high SNR, a broadband high-brightness synchrotron source is often used instead.[25,26] The synchrotron radiation based FT-IR (SR-FT-IR) spectromicroscopy has recently been successfully utilized to monitor the changing chemistry in single living bacteria during stress adaptive response[27] and in individual rod cells following exposure to intense visible white light.[28] Here, we use SR-FT-IR to monitor NGF-induced protein phosphorylation in individual living PC12 cells. PC12 cells, derived from rat pheochromocytoma, exhibit many neuron-like phenotypes upon NGF-induced differentiation.[29] The phosphorylation pathways involved in this differentiation process are well characterized. NGF triggers activation of the mitogen-activated protein kinase (MAPK) cascade in PC12 cells within minutes,[30] and continual NGF exposure leads to neuronal differentiation and sustained protein phosphorylation activities in the cells.[31] Thus, the PC12/NGF system provides us with a sustained and elevated protein phosphorylation levels that could be easily contrasted with the ground state (i.e., nondifferentiated cells). This feature in differentiated PC12 cells was used to identify the spectral changes associated with protein phosphorylation. In this study, we identified spectral markers for this protein phosphorylation feature. We also detected spectral changes in lipid and carbohydrates in parallel with the protein phosphorylation. The band assignment of the phosphorylation markers was corroborated by quantum mechanical calculations. The temporal variations of the markers correlate with the changes of protein phosphorylation levels in the cells. We further confirmed the markers' specificity by comparing FT-IR and fluorescence images of EGFP (enhanced green fluorescent protein) marked PC12 cells with sustained protein kinase activity.

EXPERIMENTAL SECTION

Cell Culture, NGF Treatment, and Sample Preparation for SR-FT-IR Spectroscopy. The rat adrenal pheochromocytoma cell line PC12 was obtained from American Type Culture Collection (ATCC, Rockville, MD). They were grown in the RPMI 1640 medium (Invitrogen, CA) supplemented with 10% horse serum, 5% fetal bovine serum (Thermo Scientific Hyclone, UT), 2 mM Glutamax (Invitrogen, CA), and in 100 mm culture dishes. They were incubated at 37 °C in a humidified atmosphere containing 7.5% CO_2. Cells were released upon confluency and plated at a density of 2×10^4 cells per gold coated glass slides (12 mm × 6 mm) which were pretreated with poly-L-lysine (PLL, Sigma-Aldrich, MO). The slides were then immersed in 4 mL of culture medium in 35 mm culture dishes for single-cell SR-FT-IR measurements and for transient transfection.

Cells plated on the gold-coated glass slides were incubated at 37 °C overnight to allow them to attach, rinsed with warm RPMI 1640 to remove nonattached cells, and incubated in the reduced-serum differentiation medium (0.67% horse serum, 0.33% fetal bovine serum) with 25 ng/mL NGF (kindly provided by the Dr. William Mobley group, University of California at San Diego). Previous studies showed that a NGF concentration of 25 ng/mL was sufficient to induce PC12 cells to differentiate (Figure 1 and see the Supporting Information). Controls were PC12 cells incubated in the NGF-free culture medium. For long-term cell culture and NGF treatment, a medium change was carried out every other day.

Immediately before the SR-FT-IR measurements, cells (on the gold-coated slides) were first rinsed with ice cold Hanks' buffered saline solution (HBSS), and the excess free-flowing

dx.doi.org/10.1021/ac300308x | Anal. Chem. 2012, 84, 4118−4125

HBSS was gently but rapidly wicked away. The slide was placed inside a microscope environmental chamber covered with a 200 nm thick infrared-transparent Si_3N_4 window. The contact between the environmental chamber and the microscope stage was tightly sealed to maintain a constant relative humidity so that the cells remained hydrated.

Transient Transfection. To induce sustained protein phosphorylation in PC12 cells, we transfected the PC12 cells with the TrkA-EGFP plasmid[33] (kindly provided by Dr. William Mobley's group), a fusion construct of TrkA (NGF receptor), and EGFP. Transient transfection of PC12 cells on a gold-coated slide was carried out using Lipofectamine 2000 (Invitrogen, CA) in Opti-MEM I reduced serum medium (Invitrogen, CA) according to manufacturer's instructions. In total, 0.25 μg of plasmid was used for each slide. The transfection efficiency for TrkA-EGFP was estimated to be less than 5%, while the efficiency for EGFP was about 60%.

SR-FT-IR Spectromicroscopy. SR-FT-IR measurements were performed using a Nicolet Magna 760 FT-IR bench model and a Nicolet Nic-Plan IR microscope with a 15×, 0.58 numerical aperture objective at the infrared Beamline 1.4.3 of the Advanced Light Source at Lawrence Berkeley National Laboratory. The IR spectra between 800 and 4000 cm^{-1} at 4 cm^{-1} resolution were recorded with 32 coadded scans. Each sample was raster scanned using the IR microscope at a 5 μm step size. These SR-FT-IR spectra from each map were exported for data processing.

Data Processing and Multivariate Analysis. For SR-FT-IR spectra that were visually free of the optical artifacts of dispersion or scattering or electric field standing wave intensity,[35−38] we used the classical "rubber band" approach to remove the baseline.[34] For spectra that visually exhibited line shape distortions due to these artifacts, we used well-established mathematical models[35−38] to separate these artifacts from pure chemical absorption. In our experience, this two-way method could minimize overcorrecting the data and avoid introducing overfitting errors. Because the dimension of the infrared beam at our experimental setup was similar to the size of a single cell,[17] each spectrum represented each single cell (see Figure S-1 in the Supporting Information). The spectra collected at the edge of cells or blank areas were filtered out automatically by setting a threshold for the amide II band strength. The band intensities were calculated by integrating the area under the IR absorption bands, above the valley-to-valley baseline, and between the two half-maximum boundaries.

Multivariate analysis methods were performed using our in-house Matlab (Mathworks, MA) programs. Principal component analysis (PCA) was applied for initial data dimension reduction. The algorithm of computing principal components (PCs) was described elsewhere.[39] We reduced the original spectra in the spectral region from 950 to 1300 cm^{-1} to 4 PCs and the corresponding scores. The first 4 PCs were selected to represent a spectrum because in total they accounted for more than 90% of the data variance (see Figure S-2 in the Supporting Information).

To separate the different spectra groups, a subsequent linear discriminant analysis (LDA) was performed on the outputs from the PCA. The PC-linear discriminants (LDs) are linear combinations of the PCs so that the projection of spectra to LDs maximizes intergroup variance and meanwhile minimizes the intragroup variance (the algorithm is described elsewhere[40]). The score plots of PC-LDA are used for visual representation of the spectra. In order to identify variables contributing to the differences between the groups in the PC-LDA score plots, a cluster vector was derived from PC-LDA loadings quantifying the contribution of each frequency to each group.[40] The cluster vectors allow one to identify the contributory frequencies that separate the different spectra groups.

Validation Experiment with Bimodal Imaging. We validated the protein phosphorylation spectral markers by using a bimodal approach (infrared and fluorescence microscopy) to image the transiently transfected PC12 cells on gold-coated slides. The infrared imaging was performed using a Thermo Nicolet Nexus 870 FT-IR bench model and a Nicolet Continuμm XL IR microscope with a 15× objective (NA 0.58) albeit with the thermal source at the infrared Beamline 1.4.4 of the Advanced Light Source because of the instrumentation availability. The Continuμm microscope was equipped with a fluorescence attachment that allows in situ fluorescence imaging on the same sample. The sample was illuminated with a high-pressure mercury burner with 100 W halogen bulb filtered through a 450−480 nm band-pass excitation filter and a 500 nm long-pass dichroic mirror. The sample fluorescence was filtered with 515 nm long-pass emission filter.

RESULTS AND DISCUSSION

SR-FT-IR Spectra of Differentiated PC12 Cells. Averaged SR-FT-IR spectrum of differentiated PC12 cells (see Figure 1A, day 7) and nontreated control cells are compared in Figure 2. (Also see Figure S-3 in the Supporting Information for the spectrum of individual cells from each group.) The two spectra are normalized to the amide II bands near 1550 cm^{-1}. While both spectra share characteristic mid-IR absorption bands from major biomolecules (summarized in Table 1), there are significant and reproducible differences between the two. In the 2800−3000 cm^{-1} region, which is associated with the aliphatic C−H stretching modes, the overall absorbance increases in differentiated PC12 cells (Figure 2,

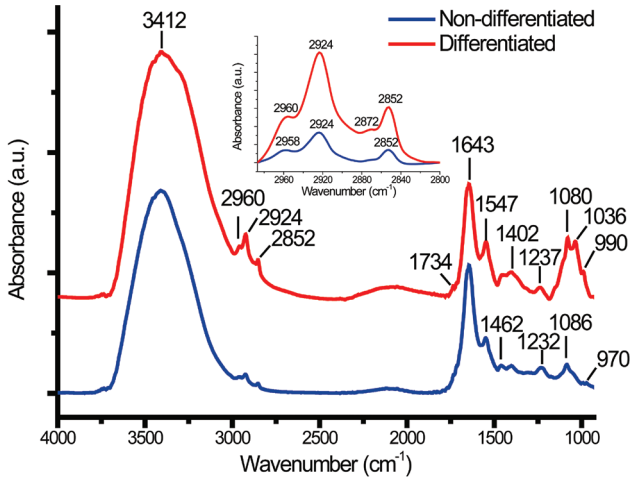

Figure 2. Comparison of typical SR-FT-IR spectra of differentiated (red) and nondifferentiated (blue) PC12 cells. The differentiated PC12 cells were treated with 25 ng/mL NGF for 7 days. The inset shows the expanded spectral region between 2800 and 3000 cm^{-1} after baseline correction. The spectra are normalized to the amide II band strength (local maximum near 1550 cm^{-1}) to normalize variations in sample biomasses.[19] See Table 1 for assignment of the marked bands.

dx.doi.org/10.1021/ac300308x | Anal. Chem. 2012, 84, 4118−4125

Table 1. Wavenumber (cm^{-1}) and Assignment of the Major Bands in the Infrared Spectra of Differentiated and Nondifferentiated PC12 Cells

wavenumber (cm^{-1})	vibrational mode assignment and main contribution
~3412	νOH of water, νNH of proteins[45]
~2960	$\nu_{as}CH_3$ of lipids, proteins and nucleic acids[42,46]
~2924	$\nu_{as}CH_2$ of lipids[42,46]
~2852	$\nu_{s}CH_2$ of lipids[42,46]
~1734	νC=O of lipids[41,47]
~1643	amide I of proteins[41,42,47,48]
~1547	amide II of proteins[41,42,47,48]
~1462	δCH_2 of lipids[46,47]
~1402	δsCH_3 of lipids and proteins and $\nu_{s}COO^-$ of amino acid side chains and fatty acids[46,47]
~1237	$\nu_{as}PO_2^-$ of nucleic acids,[47,49] lipids and phosphorylated proteins[48,50]
~1151	νC–O of protein side chain groups and carbohydrate[45,46,49]
~1080	$\nu_{s}PO_2^-$ of nucleic acids, νPO_4^{2-} of phosphorylated proteins, νC–O–C and νC–O–P of polysaccharides[48,49,51]
~1053, ~1036	νC–O coupled with δC–O of carbohydrates[45,46,52]
990–970	νPO_4^{2-} of phosphorylated proteins and nucleic acids[18,46]

inset). At ~1734 cm^{-1}, there is a concomitant rise of a shoulder band that is associated with carbonyl C=O stretching mode in non-hydrogen-bonded ester groups of phospholipids.[41] The correlated changes in these two spectral regions suggest an increase in the relative lipid to protein ratio. Furthermore, the intensity of methylene bands (~2852 and ~2924 cm^{-1}) increases more significantly than that of the methyl bands (~2872 and ~2960 cm^{-1}), indicating the ratio of the number of methylene groups to the number of methyl groups increases in differentiated cells.[42]

The most striking differences, however, are observed in the 1300–900 cm^{-1} fingerprint region, where the vibrations associated with nucleic acids, proteins, and carbohydrates are generally located. In this region, the intensity of the bands at ~1151, ~1080, ~1036, and between 990 and 970 cm^{-1} significantly increase in differentiated cells and bands appearing at ~1232 and ~1086 cm^{-1} in the control sample appear to shift to ~1237 and ~1080 cm^{-1}, respectively, in the differentiated sample. The simultaneous rise of the absorption intensities at ~1151, ~1080, and ~1036 cm^{-1} indicates an increase of carbohydrates (relative to protein content) possibly in the glycolipids and glycoproteins. This interpretation is based on the observations by Margolis et al.[43] that reported a 3-fold increase of total gangliosides and 75% increase in trypsin-releasable glycoproteins upon NGF stimulation. The increase in the absorption intensity of the ~1080 cm^{-1} band and the bands between 990 and 970 cm^{-1} might be caused by changes in the DNA/RNA phosphate backbone and/or the presence of phosphorylated proteins.[44] However, we do not expect bulk changes in DNA/RNA absorption properties because a majority of differentiated PC12 cells were arrested in the G_0/G_1 phase (Figure 1B). Furthermore, previous studies[22,41] reported a broad rise of the baseline and all bands in the 1600–1000 cm^{-1} region for cells undergoing DNA replication and mitosis in the S-phase and the G_2/M-phase, which we did not observe here. Therefore, we tentatively assign the simultaneous rises of the ~1080 cm^{-1} band and the bands between 990 and 970 cm^{-1} to the elevated protein phosphorylation status in differentiated PC12 cells. This band assignment was corroborated by calculated IR spectra of phosphorylated and nonphosphorylated amino acid residues using ab initio quantum mechanical calculations (see Figure S-4 in the Supporting Information).

Monitoring Protein Phosphorylation in Differentiating PC12 Cells over Time. After identifying the spectral differences between differentiated and nondifferentiated PC12 cells, we performed time course experiments to track spectral changes of cells during their early response periods and intermediate differentiation stages. For the time point measurements, we passaged cells from the same culture and treated them separately with NGF for different durations (see the Experimental Section). Each group of cells was prepared and measured for only one time point.

SR-FT-IR spectra were collected on cells treated with NGF for 0 (control), 2, 5, 10, 20, 40, and 60 min (named short-term treatment group hereafter) and 1, 3, 5, and 7 days (named long-term treatment group hereafter). The top panels of Figure 3A,B show a comparison of the spectra in the 1600–900 cm^{-1} region. In the short term treatment group, distinctive changes are observed in the ~1084 cm^{-1} band. In the long term treatment group, the bands at ~1036 cm^{-1} and between 990 and 970 cm^{-1} rise significantly. In addition, the 1084 cm^{-1} peak red shifts to 1080 cm^{-1} as its intensity increases, indicating a decrease in the hydrogen bonding interactions of the phosphate group.[49,53] The time courses of major absorption bands are shown in Figure 3A,B (bottom panels). During the early response periods (Figure 3A, bottom panel), the absorption bands at ~1237, ~1084, and between 990 and 970 cm^{-1} rise rapidly. Furthermore, these intensities peak at 5 min post-treatment before retreating to levels slightly higher than the ground level (i.e., the controls). The spiking behavior of these bands markedly resembles the dynamics of MAPK (aka Erk1/2) activation in PC12 cells shortly after NGF treatment (Figure 3C).

The long-term treatment group shows a second rise of phosphorylation activity 3 days after the initial peak. As shown in Figure 3B (bottom panel), the intensity of absorption bands at ~1080, ~1151, ~1036, and between 990 and 970 cm^{-1} increase appreciably during a week of NGF treatment while the ~1237 cm^{-1} band has only a mild increase. The biggest increases for these bands happened at day 3. It is of interest to note that this time point matches with the time that PC12 cells began to display extensive neurite formation (See Figure 1A). Moreover, the asymptotically increasing intensity of the bands at ~1080 and between 990 and 970 cm^{-1} reflects sustained elevated phosphorylation levels, as expected from previous literature describing long-term MAP (mitogen-activated protein) kinase and Akt activation.[31]

In summary, the results show that during both early response periods and intermediate differentiation stages there is a strong positive correlation between the intensity of bands at ~1237, ~1080, and between 990 and 970 cm^{-1} for the protein phosphorylation levels in NGF-treated PC12 cells. While the antisymmetric phosphate stretching band (~1237 cm^{-1}) responds to the variation of protein phosphorylation, it appears to be much less sensitive and less specific[18] than the symmetric phosphate stretching band (~1080 cm^{-1}). Therefore, we assign the ~1080 cm^{-1} band and the bands between ~990 and 970 cm^{-1} as spectral markers for protein phosphorylation in live PC12 cells during NGF-induced differentiation.

Statistical Significance of the Spectral Features during PC12 Differentiation. To evaluate the statistical

dx.doi.org/10.1021/ac300308x | Anal. Chem. 2012, 84, 4118–4125

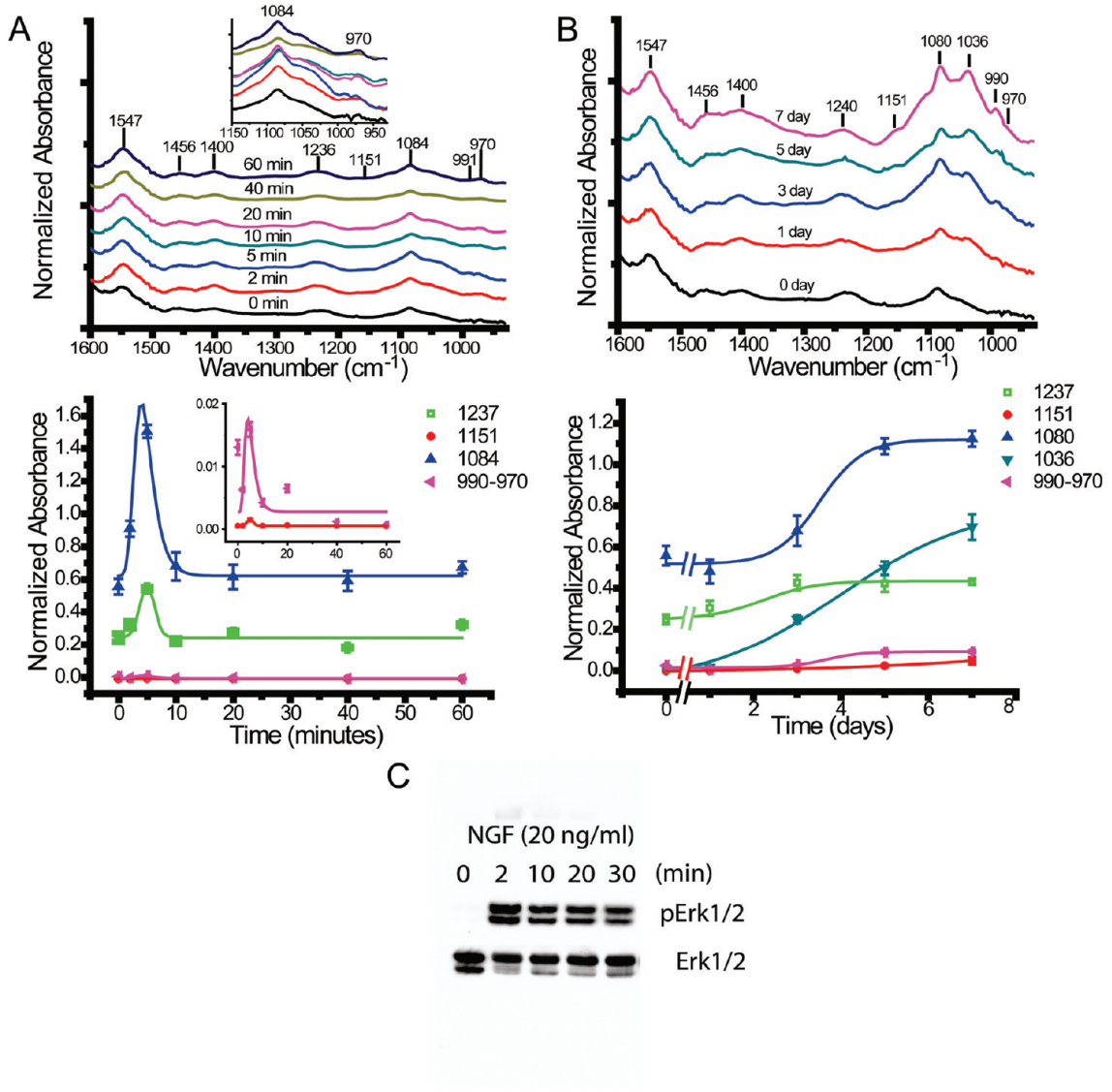

Figure 3. Progressive spectral changes in the fingerprint region during PC12 cell differentiation. (A) Changes during the first hour of NGF treatment. (Top) The mean FT-IR spectra for each time point are averaged over 150 cells (n = 150). Inset: enlarged spectrum in the 1150–900 cm^{-1} region. (Bottom) The intensity curves of prominent IR bands. The trend lines were fitted to the experimental data using nonlinear curve fit methods. Error bars represent the standard error of the mean (SEM). Inset: enlarged curves of the 1151 and 990–970 cm^{-1} bands. (B) Changes during a 7-day NGF treatment. (Top) The mean FT-IR spectra of each time point. (Bottom) The intensity curves of prominent IR bands during 7 days of NGF treatment. n = 150; error bars represent SEM. The short-term data points (within the first hour) are not replotted here. All band intensities were calculated by integrating the normalized spectra (i.e., normalized to the amide II band peak at near 1550 cm^{-1}). (C) Western blot of pErk1/2 (phosphorylated Erk1/2) and total Erk1/2 protein levels in PC12 cells after treatment with 20 ng/mL NGF for the indicated time periods. The pErk1/2 level increases significantly at 2 min and gradually decreases from 10 to 30 min. The total Erk1/2 blot shows equal loading of Erk1/2 proteins.

significance of the observed spectral changes, we performed principal component analysis in conjunction with linear discriminant analysis (PC-LDA) on spectra data in the fingerprint region from 950 to 1300 cm^{-1}. The PC-LDA score plots of the short-term and long-term treatment groups are shown in Figure 4A,B. Among the short-term treatment groups (Figure 4A, top panel), the distance between the control and the treated groups is the largest for the 5 min treatment groups, which started to decrease after 10 min of treatment. As discussed earlier, this temporal behavior possibly reflects the rapid initial rise that was followed by a gradual fall of protein phosphorylation levels in the PC12 cell upon NGF stimulation within the first hour. The score plots of the 2 min, 20 min, and 60 min treated groups partially overlap. Together with the earlier time-course spectral analysis, we interpret this as an indicator that chemical changes in PC12 cells during this early period could be partly reversible. This is supported by our observation that the morphology of the PC12 cells returned to the original state (e.g., the retraction of the neurites) when NGF was withdrawn before 72 h.

The PC-LDA score plots of the long-term treatment groups, as shown in Figure 4B (top panel), are located further away from the control group, and all five groups (0, 1, 3, 5, and 7 days) are distinctly separated from each other. Moreover, it appears that the distances between the treated groups and the control group increase with the treatment time. This further demonstrates that the spectral changes in long-term treated

dx.doi.org/10.1021/ac300308x | Anal. Chem. 2012, 84, 4118–4125

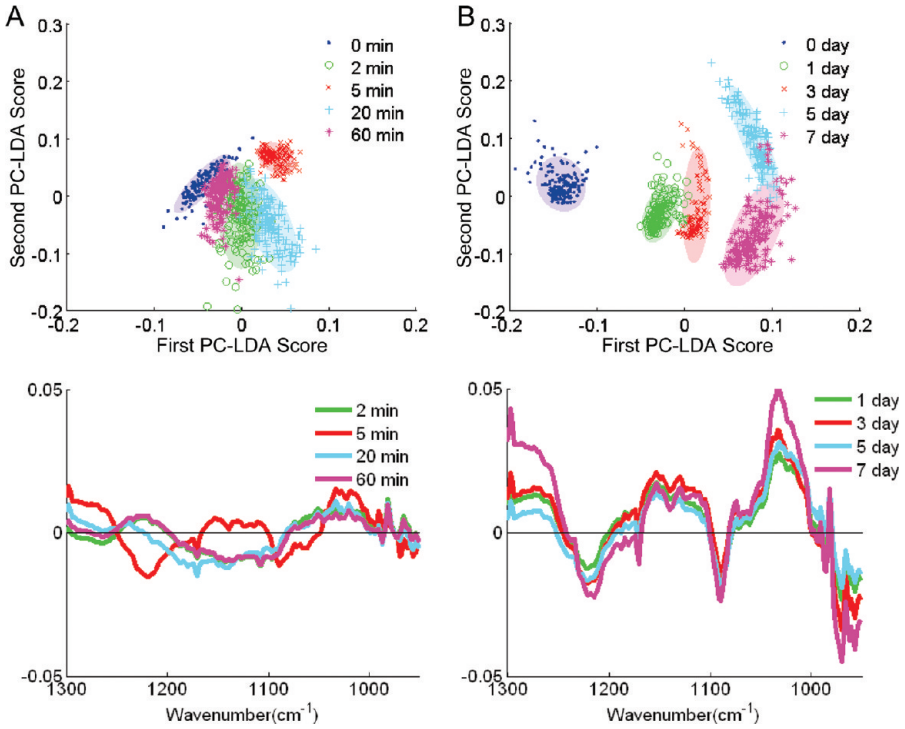

Figure 4. PC-LDA of FT-IR spectra of NGF-treated PC12 cells. (A) (Top) 2-Dimensional PC-LDA score plots of selected short-term treated groups, by projecting spectra in the direction of the first and second PC-LDA factors; n = 150, each ellipse covers an area of 95% confidence level. (Bottom) Difference PC-LDA cluster vectors for representative short-term treated groups. (B) (Top) PC-LDA score plots of long-term treated cells. Each ellipse covers an area of 95% confidence level. (Bottom) Difference PC-LDA cluster vectors for representative long-term treated groups.

PC12 cells are correlated with the progression of cell differentiation, and the changes are irreversible.

To determine which variables are accountable for the group separation, we calculated the cluster vectors of each group.[40] In order to identify biochemical alterations between the treated and the control group, we computed the difference of the cluster vector between the treated and the control groups, which are shown in Figure 4A,B (the bottom panels), respectively. The contributing bands are mainly associated with protein phosphorylation (in regions of 990−970, 1090−1080, and 1240−1220 cm^{-1}) and carbohydrates (~1030, ~1130, ~1153, and ~1171 cm^{-1}). This confirms that the spectral differences among NGF-treated cells were statistically significant, and the marker bands associated with protein phosphorylation are contributors to the separation of the groups.

Validation of Spectral Markers for Protein Phosphorylation Using Bimodal Imaging. To confirm the specificity of the marker bands for protein phosphorylation in live PC12 cells, we performed bimodal (infrared spectromicroscopy/fluorescent microscopy) imaging on the PC12 cells which were transfected with the TrkA-EGFP fusion plasmid (see the Experimental Section). Overexpressing TrkA leads to receptor autophosphorylation and the sustained activity of several cellular protein kinases, such as Erk1 and PI-3 kinase in PC12 cells.[54] The coexpressed EGFP protein served as a fluorescent marker for transfected PC12 cells with sustained protein kinase activity.

Figure 5A shows the bright field, fluorescence, and infrared images of a cluster of monolayer transfected PC12 cells. The infrared images of ~2924 and ~1550 cm^{-1} bands, dominated by lipid and protein signal, respectively, identify the location of the PC12 cells. The bright spots in the infrared image of the ~1080 cm^{-1} band and the bands between 990 and 970 cm^{-1} are colocalized with the green fluorescent spots (marked by white arrows) in the fluorescence image.

In control experiments (Figure 5B), PC12 cells were transfected with an EGFP plasmid. In the absence of additional TrkA expression, there was minimal colocalization of spatial features between the infrared and the fluorescence images, further confirming the specificity of the correlation between the intensity of ~1080 cm^{-1} bands and the bands between 990 and 970 cm^{-1} and protein phosphorylation levels.

CONCLUSIONS

We have demonstrated and confirmed that SR-FT-IR spectromicroscopy can be used to measure protein phosphorylation. We used SR-FT-IR to identify statistically significant spectral changes in individual PC12 cells during NGF-induced differentiation and were able to detect a multistage phosphorylation process during the first week of the neuronal differentiation of PC12 cells. Considering the complexity of a living mammalian cell system, the temporal consistency of those spectral changes with the variation of protein phosphorylation levels in the cells is remarkable. These results open up new possibilities to noninvasively monitor ongoing intracellular phosphorylation processes in a wide variety of cellular activities in real-time. To this end, our lab is currently building an IR-compatible microfluidic mammalian cell culture device, which can maintain living cells in aqueous media on a microscope stage during continuous data acquisition.

In addition to shedding new light on the dynamics of protein phosphorylation processes, the SR-FT-IR technique also enables us to identify the parallel changes of lipids and carbohydrates composition in differentiated PC12 cells. The multimolecule sensitivity of this technique thus offers a unique

dx.doi.org/10.1021/ac300308x | Anal. Chem. 2012, 84, 4118−4125

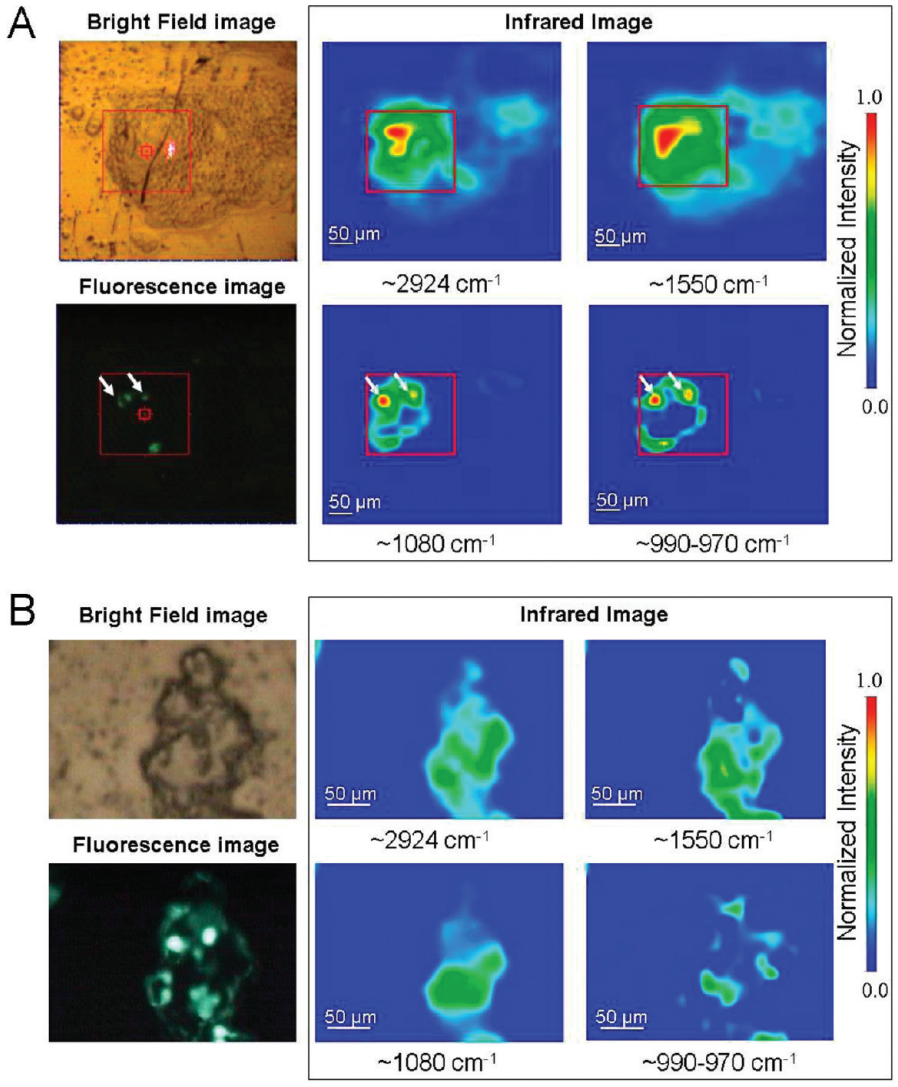

Figure 5. Validation with bimodal imaging. (A) In situ bimodal registration of phosphorylation in PC12 cell clusters transfected with TrkA-EGFP fusion plasmid. The bright field image and the fluorescence image were obtained from the same cluster of TrkA-EGFP transfected PC12 cells at the same time. The infrared images are intensity maps for the corresponding infrared bands as annotated in the figure. The ~2914 cm^{-1} band is associated with lipids, and the ~1550 cm^{-1} band is associated with proteins (see Table 1). The bands between 990 and 970 cm^{-1} are integrated together. The large red squares mark the region of interest. The white arrows indicate the location of transfected cells (green fluorescent spots) and the corresponding spots in the infrared map. The bright fluorescent spot at the lower edge does not register in any of the four infrared images. It may come from nonspecific autofluorescence of necrotic cells. (B) The corresponding bright field, fluorescence, and infrared images of a PC12 cell cluster transfected only with EGFP.

multiplexing capability to simultaneously monitor parallel biochemical changes during cellular signaling processes in response to external stimulation.

■ ASSOCIATED CONTENT

Supporting Information

Additional information as noted in text. This material is available free of charge via the Internet at http://pubs.acs.org.

■ AUTHOR INFORMATION

Corresponding Author

*Address: Hoi-Ying N. Holman, Ph.D. Mailstop: 70A-3317L, Lawrence Berkeley National Laboratory, 1 Cyclotron Road, Berkeley, CA 94720. Phone: (510) 486-5943. E-mail: hyholman@lbl.gov. Address: Steven Chu, Ph.D. U.S. Department of Energy 1000 Independence Ave., SW Washington, DC 20585. Phone: (202) 586-6210. Fax: (202) 586-4403.

Present Address

⊥U.S. Department of Energy, 1000 Independence Ave., SW, Washington, DC 20585.

Notes

The authors declare no competing financial interest.

■ ACKNOWLEDGMENTS

We are grateful to Dr. Eleanor Blakely and Ms. Kathleen Bjornstad for generously making tissue culture facilities available, and Dr. William Mobley's group for supplying some of the key reagents. This work was supported by the Berkeley Synchrotron Infrared Structural Biology (BSISB) program and by the U.S. Department of Energy Office of Biological and Environmental Research's Structural Biology Program through Contracts DE-AC02-05CH11231 and KP1501021 with Lawrence Berkeley National Laboratory. The Advanced Light Source is supported by the Director, Office of Science, Office of

Basic Energy Sciences, of the U.S. Department of Energy under Contract No. DE-AC02-05CH11231.

REFERENCES

(1) Manning, G.; Whyte, D. B.; Martinez, R.; Hunter, T.; Sudarsanam, S. *Science* **2002**, *298* (5600), 1912−1934.
(2) Manning, G.; Plowman, G. D.; Hunter, T.; Sudarsanam, S. *Trends Biochem. Sci.* **2002**, *27* (10), 514−520.
(3) Watson, F. L.; Heerssen, H. M.; Bhattacharyya, A.; Klesse, L.; Lin, M. Z.; Segal, R. A. *Nat. Neurosci.* **2001**, *4* (10), 981−988.
(4) Liu, L.; Cundiff, P.; Abel, G.; Wang, Y.; Faigle, R.; Sakagami, H.; Xu, M.; Xia, Z. *Proc. Natl. Acad. Sci. U.S.A.* **2006**, *103* (25), 9697−9702.
(5) Ross, A. H.; Baltimore, D.; Eisen, H. N. *Nature* **1981**, *294* (5842), 654−656.
(6) Ciaccio, M. F.; Wagner, J. P.; Chuu, C. P.; Lauffenburger, D. A.; Jones, R. B. *Nat. Methods* **2010**, *7* (2), 148−155.
(7) Stukenberg, P. T.; Fuller, B. G.; Lampson, M. A.; Foley, E. A.; Rosasco-Nitcher, S.; Le, K. V.; Tobelmann, P.; Brautigan, D. L.; Kapoor, T. M. *Nature* **2008**, *453* (7198), 1132−U14.
(8) Randriamampita, C.; Mouchacca, P.; Malissen, B.; Marguet, D.; Trautmann, A.; Lellouch, A. C. *PLoS One* **2008**, *3*, 1.
(9) Zhang, J.; Hupfeld, C. J.; Taylor, S. S.; Olefsky, J. M.; Tsien, R. Y. *Nature* **2005**, *437* (7058), 569−573.
(10) Matsuda, M.; Aoki, K.; Kiyokawa, E.; Nakamura, T. *Phil. Trans. R. Soc. B: Biol. Sci.* **2008**, *363* (1500), 2143−2151.
(11) Shachaf, C. M.; Elchuri, S. V.; Koh, A. L.; Zhu, J.; Nguyen, L. N.; Mitchell, D. J.; Zhang, J. W.; Swartz, K. B.; Sun, L.; Chan, S.; Sinclair, R.; Nolan, G. P. *PLoS One* **2009**, *4*, 4.
(12) Kneipp, K.; Haka, A. S.; Kneipp, H.; Badizadegan, K.; Yoshizawa, N.; Boone, C.; Shafer-Peltier, K. E.; Motz, J. T.; Dasari, R. R.; Feld, M. S. *Appl. Spectrosc.* **2002**, *56* (2), 150−154.
(13) Jell, G.; Swain, R. ; Stevens, M. M. Raman Spectroscopy: A Tool for Tissue Engineering. In *Emerging Raman Applications and Techniques in Biomedical and Pharmaceutical Fields*; Matousek, P., Morris, M. D., Eds.; Springer Science+Business Media: Berlin, Heildelberg, Germany, 2010; pp 419−437.
(14) Huang, Y. S.; Karashima, T.; Yamamoto, M.; Hamaguchi, H. O. *Biochemistry* **2005**, *44* (30), 10009−10019.
(15) van Manen, H. J.; Lenferink, A.; Otto, C. *Anal. Chem.* **2008**, *80* (24), 9576−9582.
(16) Holman, H. Y. N.; Martin, M. C.; McKinney, W. R. *J. Biol. Phys.* **2003**, *29* (2−3), 275−286.
(17) Holman, H. Y. N.; Bechtel, H. A.; Hao, Z.; Martin, M. C. *Anal. Chem.* **2010**, *82* (21), 8757−8765.
(18) Sanchez-Ruiz, J. M.; Martinez-Carrion, M. *Biochemistry* **1988**, *27* (9), 3338−3342.
(19) Barth, A.; Mantele, W. *Biophys. J.* **1998**, *75* (1), 538−44.
(20) Katsunori, I.; Sachiko, S. Y.; Kunihiro, C.; Kunio, A. In *FT-IR Analysis of Phosphorylated Protein*; Michel, D. F., Patrick, M., Eds.; SPIE: Bellingham, WA, 2004; pp 17−21.
(21) Miller, L. M.; Dumas, P. *Biochim. Biophys. Acta* **2006**, *1758* (7), 846−857.
(22) Diem, M.; Romeo, M.; Matthaus, C.; Miljkovic, M.; Miller, L.; Lasch, P. *Infrared Phys. Technol.* **2004**, *45* (5−6), 331−338.
(23) Miljkovic, M.; Romeo, M.; Matthaus, C.; Diem, M. *Biopolymers* **2004**, *74* (1−2), 172−175.
(24) Kuimova, M. K.; Chan, K. L.; Kazarian, S. G. *Appl. Spectrosc.* **2009**, *63* (2), 164−171.
(25) Nasse, M. J.; Walsh, M. J.; Mattson, E. C.; Reininger, R.; Kajdacsy-Balla, A.; Macias, V.; Bhargava, R.; Hirschmugl, C. J. *Nat. Methods* **2011**, *8* (5), 413−416.
(26) Dumas, P.; Sockalingum, G. D.; Sule-Suso, J. *Trends Biotechnol.* **2007**, *25* (1), 40−44.
(27) Holman, H. Y.; Wozei, E.; Lin, Z.; Comolli, L. R.; Ball, D. A.; Borglin, S.; Fields, M. W.; Hazen, T. C.; Downing, K. H. *Proc. Natl. Acad. Sci. U.S.A.* **2009**, *106* (31), 12599−12604.
(28) Quaroni, L.; Zlateva, T.; Normand, E. *Anal. Chem.* **2011**, *83* (19), 7371−7380.
(29) Fujita, K.; Lazarovici, P.; Guroff, G. *Environ. Health Perspect.* **1989**, *80*, 127−142.
(30) Gomez, N.; Cohen, P. *Nature* **1991**, *353* (6340), 170−173.
(31) Chang, J. H.; Mellon, E.; Schanen, N. C.; Twiss, J. L. *J. Biol. Chem.* **2003**, *278* (44), 42877−42885.
(32) Van Buskirk, R. G.; Gabriels, J.; Wagner, J. *In Vitro Cell. Dev. Biol.* **1988**, *24* (5), 451−6.
(33) Jullien, J.; Guili, V.; Derrington, E. A.; Darlix, J. L.; Reichardt, L. F.; Rudkin, B. B. *J. Biol. Chem.* **2003**, *278* (10), 8706−8716.
(34) Wartewig, S., *IR and Raman Spectroscopy:Fundamental Processing*; Wiley-VCH: Weinheim, Germany, 2003.
(35) Mohlenhoff, B.; Romeo, M.; Diem, M.; Wood, B. R. *Biophys. J.* **2005**, *88* (5), 3635−3640.
(36) Bassan, P.; Kohler, A.; Martens, H.; Lee, J.; Byrne, H. J.; Dumas, P.; Gazi, E.; Brown, M.; Clarke, N.; Gardner, P. *Analyst* **2010**, *135* (2), 268−277.
(37) Bassan, P.; Byrne, H. J.; Bonnier, F.; Lee, J.; Dumas, P.; Gardner, P. *Analyst* **2009**, *134* (8), 1586−1593.
(38) Filik, J.; Frogley, M. D.; Pijanka, J. K.; Wehbe, K.; Cinque, G. *Analyst* **2012**, *137* (4), 853−861.
(39) Esbensen, K. H., *Multivariate Data Analysis in Practice*, 5th ed.; CAMO Process AS: Woodbridge, NJ, 2004.
(40) Martin, F. L.; German, M. J.; Wit, E.; Fearn, T.; Ragavan, N.; Pollock, H. M. *J. Comput. Biol.* **2007**, *14* (9), 1176−1184.
(41) Holman, H. Y.; Martin, M. C.; Blakely, E. A.; Bjornstad, K.; McKinney, W. R. *Biopolymers* **2000**, *57* (6), 329−335.
(42) Wong, P. T. T.; Lacelle, S.; Fung, M. F. K.; Senterman, M.; Mikhael, N. Z. *Biospectroscopy* **1995**, *1* (5), 357−364.
(43) Margolis, R. K.; Salton, S. R. J.; Margolis, R. U. *J. Biol. Chem.* **1983**, *258* (7), 4110−4117.
(44) Tobin, M. J.; Chesters, M. A.; Chalmers, J. M.; Rutten, F. J.; Fisher, S. E.; Symonds, I. M.; Hitchcock, A.; Allibone, R.; Dias-Gunasekara, S. *Faraday Discuss.* **2004**, *126*, 27−39 ; discussion 77−92.
(45) Parker, F. S. *Applications of Infrared Spectroscopy in Biochemistry, Biology, And Medicine*. Plenum Press: New York, 1971; p xiv, 601.
(46) Maziak, D. E.; Do, M. T.; Shamji, F. M.; Sundaresan, S. R.; Perkins, D. G.; Wong, P. T. *Cancer Detect. Prev.* **2007**, *31* (3), 244−253.
(47) Jamin, N.; Miller, L.; Moncuit, J.; Fridman, W. H.; Dumas, P.; Teillaud, J. L. *Biopolymers* **2003**, *72* (5), 366−373.
(48) Lasch, P.; Pacifico, A.; Diem, M. *Biopolymers* **2002**, *67* (4−5), 335−338.
(49) Wong, P. T.; Wong, R. K.; Caputo, T. A.; Godwin, T. A.; Rigas, B. *Proc. Natl. Acad. Sci. U.S.A.* **1991**, *88* (24), 10988−10992.
(50) Bonda, M.; Perrin, V.; Vileno, B.; Runne, H.; Kretlow, A.; Forro, L.; Luthi-Carter, R.; Miller, L. M.; Jeney, S. *Anal. Chem.* **2011**, *83*, 7712−7720.
(51) Holman, H. Y.; Miles, R.; Hao, Z.; Wozei, E.; Anderson, L. M.; Yang, H. *Anal. Chem.* **2009**, *81* (20), 8564−8570.
(52) Liu, M. J.; Wang, Z.; Wu, R. C.; Sun, S. Q.; Wu, Q. Y. *Leukemia* **2003**, *17* (8), 1670−1674.
(53) Rigas, B.; Wong, P. T. *Cancer Res.* **1992**, *52* (1), 84−88.
(54) Hempstead, B. L.; Rabin, S. J.; Kaplan, L.; Reid, S.; Parada, L. F.; Kaplan, D. R. *Neuron* **1992**, *9* (5), 883−896.